Detecting delocalization†

Adam J. Bridgeman*[a] and Christopher J. Empson[b]

Received (in Durham, UK) 22nd January 2008, Accepted 27th February 2008
First published as an Advance Article on the web 15th April 2008
DOI: 10.1039/b801180j

As the bonding in many compounds can be adequately described using localized, two-centre two-electron bonds, the electronic structure of molecules where such a description is inadequate is often chemically very interesting. Three-centre bond orders provide a useful tool for detecting the presence and analyzing the importance of multicentre and hypervalent effects. To depict the resulting chemical structures, a graphical device is introduced which constructs the chemical connections *ab initio* from the electronic structure. The three-centre, two-electron bonding in a set of electron-deficient boranes and the three-centre, four-electron bonding in a set of electron-rich xenon fluorides has been analyzed and the approach has been used to test for the occurrence and importance of *pseudo*-aromatic, closed-loops in polyoxometalates.

Introduction

Prior to the introduction of the concept of multicentre bonding by Lipscomb,[1–3] Pauling,[4] Wade[5] and others,[5,6] chemical bonding in stable compounds was considered to be limited to two-centre interactions. These were described by the traditional Lewis bond multiplicity based on sharing electron pairs with every atom possessing a complete 'octet' of valence electrons.[7,8] In many ways, the Lewis model has survived the advent of quantum mechanics with the electron-pairs being replaced by doubly occupied molecular orbitals or localized 'bond orbitals'.

In this paper, we show how the presence and importance of multicentre and hypervalent interactions can be analyzed. A graphical device is introduced which is used to detect these effects. The approach is illustrated with reference to the electron deficiency in boranes and delocalization in electron-rich xenon fluorides and polyoxometalates.

Modern electronic structure theory however focuses, almost completely, on molecular orbitals (MOs) and electron densities which are delocalized over the entire molecule. The connection between Lewis structures and these functions is not at all obvious and many attempts have been made to make such links. We have previously shown, for example, the usefulness of calculating bond orders either between atomic pairs[9] or between molecular fragments.[10]

In most molecules the bonding can be adequately described in terms of the electron pair, two-centre two-electron (2c-2e) bonds of the Lewis model. In such cases, as illustrated in Scheme 1 for methane, the molecular orbitals can be transformed into localized molecular orbitals (LMOs) which resemble Lewis structures.

Such localization procedures[11] are possible in many molecules but do not always yield orbitals which resemble the 'traditional' chemist's view of the bonding: in ethene, two C–H bonding orbitals and two bent C–C bonding orbitals result. These 'banana bonds' are curved between each centre rather than the σ- and π-forms usually drawn which, in fact, more closely resemble the delocalized forms.

It is not always possible to transform delocalized molecular orbitals into localized '2c-2e' orbitals and the bonding in such molecules is often chemically very interesting. In benzene, the π-orbitals can be localized only over a minimum of three atoms. In diborane, localization of the molecular orbitals produces localized B–H σ-bonding orbitals for each terminally attached hydrogen atom and two orbitals of the type illustrated in Scheme 2. Each of the latter involves one of the bridging hydrogen atoms and both boron atoms and are commonly taken to represent three-centre two-electron bonds (3c-2e). Although constructed from the delocalized molecular orbitals by a localization procedure, they are commonly referred to as delocalized, multicentre bonds.

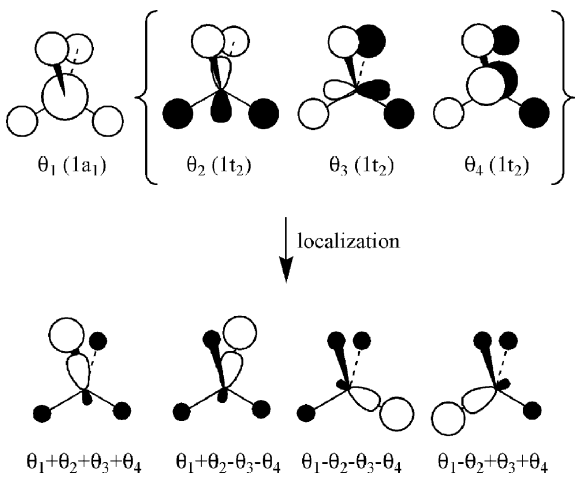

Scheme 1 Transformation of delocalized molecular orbitals into C–H bond orbitals in methane.

[a] *School of Chemistry, University of Sydney, Sydney Australia. E-mail: A.Bridgeman@chem.usyd.edu.au; Fax: +61 (0)2 93513329; Tel: +61 (0)2 93512731*
[b] *Department of Chemistry, University of Hull, Kingston-upon-Hull, UK HU6 7RX*

† Electronic supplementary information (ESI) available: Optimized and experimentally available structures for the boranes and xenon fluorides, See DOI: 10.1039/b801180j

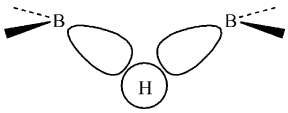

Scheme 2 3c-2e B–H–B bonding orbital in B_2H_6.

The bonding in the archetypical hypervalent molecule XeF_2 can be most simply described using only the p orbitals of the central atom. Localization of the two σ-orbitals, illustrated in Scheme 3, leads to functions which are *not* Xe–F localized electron pair bonding functions. The contribution of the Xe $5p_\sigma$ orbital is divided between the two localized functions so that each is actually a $\frac{1}{2}$ bond. The four electrons in the delocalized orbitals are thus commonly referred to as forming a three-centre four-electron bond (3c-4e). It is not possible to localize the bonding to make 2c-2e Xe–F single bonds.

The vast majority of the literature concerning multicentre bonding is devoted to discussion of three-centre interactions, as most localization procedures tend to show the low importance of higher interactions. A number of studies have investigated higher order four-,[12–14] five-[15,16] and six-centre[12,15,16] bonding interactions, though the practical utility of quantifying multicentre bonds involving more than three atoms is rather limited.

Commonly, three-centre bonds involve either one pair of electrons, resulting in a three-centre two-electron (3c-2e) bond, or two pairs of electrons, forming a three-centre four-electron (3c-4e) bond. 3c-2e bonds are mainly associated with electron-deficient molecules such as boranes, where they maximize the bonding potential of the available valence electrons. 3c-4e bonds have been proposed in hypervalent molecules.

The LMOs produced by localization schemes are not unique and tails in them, such as those evident even for the simple methane molecule in Scheme 1, can make assignment to a particular pair of atoms ambiguous. Two quite different approaches are available to enable the chemist to identify and quantify the extent of multicentre bonding within a given molecule. In the topological 'atoms in molecules' (AIM)[17] approach, the number of electrons participating in a bond is used to characterize 3c-2e bonds and this approach has applied to some electron-deficient molecules such as the boranes.[18,19]

An analysis based on delocalized orbitals is often more transparent when discussing reactivity and in showing the connections between apparently unrelated systems and can utilize the symmetry of molecules. For the analysis of two-

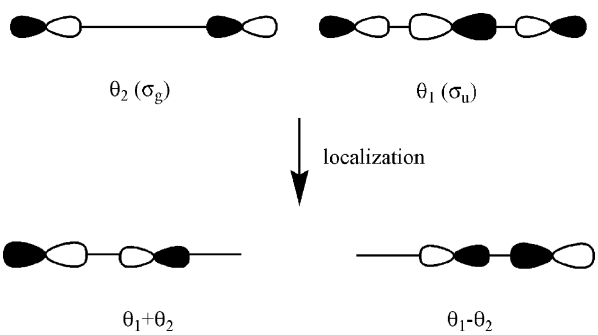

Scheme 3 Transformation of delocalized molecular orbitals into Xe–F $\frac{1}{2}$ bond orbitals in XeF_2.

centre bonding in inorganic molecules[9] and clusters,[20,21] we have found the bond order due to Mayer,[22,23] itself a generalization of the definitions by Wiberg[24] and Armstrong *et al.*[25] to be particularly useful. The bond order, β_{AB}, between two atoms A and B is given by:

$$\beta_{AB}(AO) = \sum_{i}^{\text{on A}} \sum_{j}^{\text{on B}} (PS)_{ij}(PS)_{ji} \qquad (1)$$

where **P** and **S** are the density and overlap matrices and the summations run over the atomic orbitals (AOs) centred on the two atoms. The total 'bonding power' or valency, V_A, of atom A has been defined[26] as a combined measure of covalent (covalency) and ionic (electrovalent) bonding:

$$V_A = \tfrac{1}{2}[C_A + (C_A + 4Q_A^2)]^{\frac{1}{2}} \qquad (2)$$

where the covalency, C_A, is the sum of the two-centre bond orders involving the atom and Q_A is its Mulliken charge.

We have recently shown[10] how this definition can be usefully extended to non-atomic fragments, allowing the bonding in sandwich complexes, for example, to be analyzed in terms of metal–ring interactions. The two-centre bond order can be readily extended to define multicentre indices, such as the three centre bond order:[27–31]

$$\beta_{ABC}(AO) = \sum_{i}^{\text{on A}} \sum_{j}^{\text{on B}} \sum_{k}^{\text{on C}} (PS)_{ij}(PS)_{jk}(PS)_{ki} \qquad (3)$$

Molecular orbital calculations yield positive bond orders for 3c-2e interactions, whereas they yield negative values for 3c-4e bonds.[32] The magnitude of interaction that constitutes a genuine three-centre bond has been debated in the literature. For 3c-2e interactions a bond order $\beta_{ABC} \geq 0.1$ is regarded as significant,[28] whereas for 3c-4e bonds there is debate surrounding what bond order should be considered statistically significant. Ponec *et al.* go as far as to assert[33] that 3c-4e bonding, "does not represent a real bonding mechanism", at least in relation to the species studied.

Computational approach

Geometry optimizations have been carried out using the BP86[34–36] density functional approach using the ADF program[37–39] with triple-ζ (TZ2P) Slater-type orbital basis sets and incorporating frozen cores (ADF TZP B.1s, O.1s, F.1s, Nb.3d, Mo.3d, Xe.4d) and the ZORA relativistic correction. Two- and three-centre bond orders were calculated from ADF output using the definitions given in eqn (1) and (2) with an extended version of our *MAYER* software.[40]

Visualization

In the Lewis structures of simple molecules, the bond multiplicity is represented by the number of solid lines between pairs of atoms. When non-integral bond orders or delocalized bonds have to be ascribed, dotted lines are often used. For systems containing multicentre interactions, the interacting centres are sometimes joined by intersecting lines leading to often complex diagrams. Chemists usually use their own experience and perceived knowledge of bonding rules when

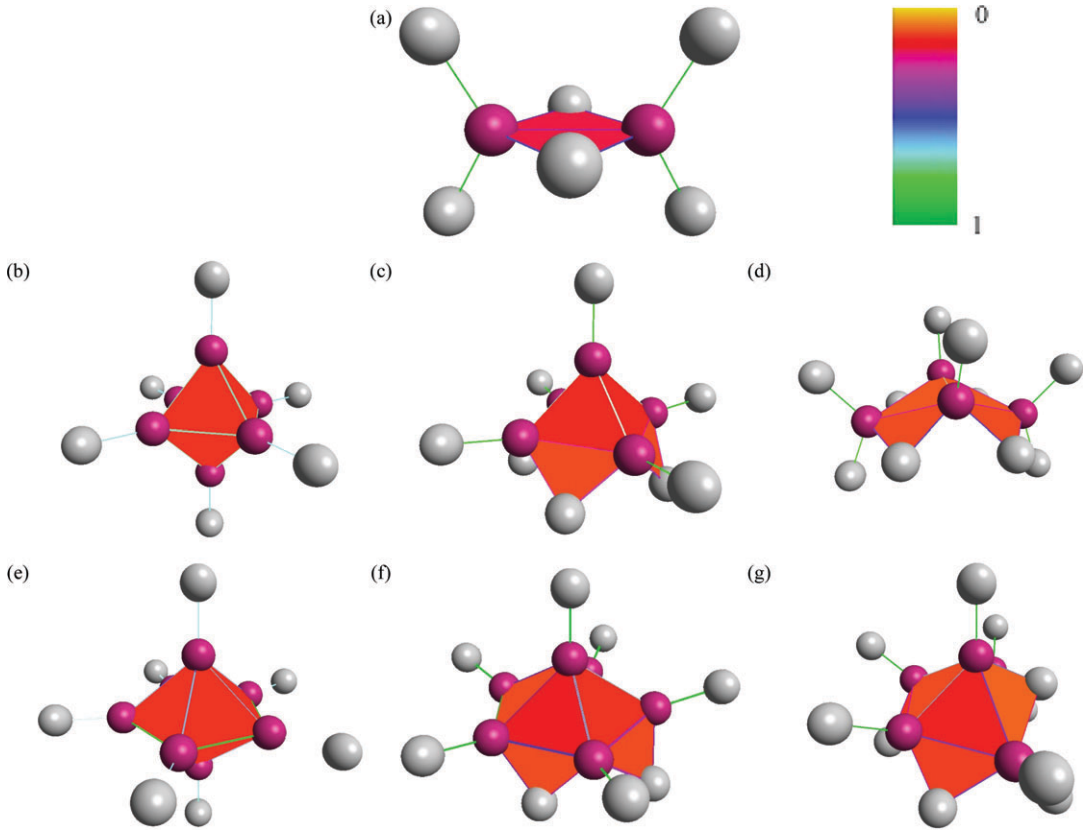

Fig. 1 Molecular diagrams for (a) B_2H_6, (b) $[B_6H_6]^{2-}$, (c) B_5H_9, (d) B_4H_{10}, (e) $[B_7H_7]^{2-}$, (f) B_6H_{10} and (g) B_5H_{11} showing two-centre bond orders as coloured lines and three-centre bond orders as coloured triangles using the colour scale shown.

constructing molecular diagrams. Chemical modelling and drawing software typically decides on the presence or absence of bonds using algorithms based on the interatomic spacing. Both approaches are prone to bias and may not be appropriate when the bonding is complex.

A two-centre bond order analysis gives information on the interactions between every pair of atoms in a molecule and thus allows the chemical topology to be described. Similarly, an analysis of multicentre bonding gives information on the presence and importance of the delocalized bonding between sets of atoms. In this paper, the chemical diagrams are constructed *ab initio* from the electronic structure calculations. The *MAYER VISUALIZER* software[41] is a computational chemistry tool for visualizing the results of bond order calculations. As in the classical representation, two-centre interactions are shown using a line but a colour scale is used to represent the bond order. Similarly, three-centre interactions are shown with coloured triangles.

This approach allows all possible interactions to be represented without recourse to the chemical experience of the user and uses a more direct measure of chemical interaction than the bond length. *Via* a bond order analysis, the atom–atom connections in the optimized structure are made *ab initio*.

Multicentre bonding in electron-deficient compounds

The large class of compounds known as boranes are probably the most familiar electron-deficient compounds. They are characterized by having structures based on polyhedra with triangular faces and can contain both terminal (H_t) and bridging (H_b) hydrogen atoms. In this work, we explore the conclusions reached by Housecroft *et al.*[42] and Armstrong *et al.*[43] on the bonding patterns in the *closo* boranes and extend this study to the *nido* and *arachno* systems. By extending the studies of these workers to multicentre interactions, the present work aims to investigate both the importance of three-centre interactions and their influence on the two-centre terms. The optimized and available experimental structures are given in the ESI.† Fig. 1 shows the calculated molecular diagrams for the systems analyzed which may be compared with the classic analyses of Wade[44] and Williams[45] of structural patterns.

The 3c-2e B–H_b–B bonding in the smallest member, diborane, has been extensively studied computationally[18,19,29,31,46] and serves as a familiar introduction to multicentre bonding in undergraduate textbooks. Three-centre B–H_b–B interactions are detected ($\beta_{BH_bB} = 0.20$) but all other possible multicentre interactions are negligible. A significant two-centre B–B link ($\beta_{BB} = 0.43$) is also calculated. Localization does not indicate the presence of a B–B bond and the apparent two-centre bond order can be seen to arise only *via* the three-centre B–H_b–B interaction. The higher-order bond order modifies the lower-order term[28] and two-centre bond orders should not be interpreted as evidence of localized interactions in the absence of a higher-order analysis. The calculated molecular diagram for diborane in Fig. 1(a) conveniently summarizes these results

and shows the presence and relative importance of the two- and three-centre interactions. The relatively small B–B separation leads standard molecular drawing software to draw a bond between the boron atoms. The more complete bond order analysis shows the true source of the interaction. Hexaborane(6), $B_6H_6^{2-}$, is an octahedral *closo* borane with localized 2c-2e B–H_t at each vertex. The edge bond order (β_{BB} = 0.68) is in excellent agreement with the bond indices calculated by Housecroft *et al.*[42] using the CNDO-SCF approach. The cross-polyhedral B–B bond orders (β_{BB} = 0.12) also provide a significant contribution to the overall bonding. Eight 3c-2e B_3 bonds are detected on each face (β_{BBB} = 0.15). No other significant three-centre interactions are found and the molecular diagram in Fig. 1(b) concurs with the suggestion by Housecroft *et al.* that the skeletal electron density lies on the *pseudo*-spherical surface which connects the boron atoms.[42]

Pentaborane(9), B_5H_9, is a square-pyramidal, *nido* borane. The B_{ax}–B_{eq} distances are *ca.* 0.1 Å shorter than the B_{eq}–B_{eq} distances and have markedly larger bond orders ($\beta_{B_{ax}B_{eq}}$ = 0.70 and $\beta_{B_{eq}B_{eq}}$ = 0.40). The four B_3 triangular faces in B_5H_9 are characterized by 3c-2e bonds (β_{BBB} = 0.15), suggesting that the cluster bonding network in B_5H_9 and $B_6H_6^{2-}$ is not greatly disrupted by removal of a boron vertex. The only other significant three-centre bonds are four B_{eq}–H_b–B_{eq} (β_{BH_bB} = 0.15) interactions which appear to be slightly weaker than those in B_2H_6. The molecular diagram in Fig. 1(c) thus describes the *nido* surface in an analogous manner to hexaborane(6). Tetraborane(10) (B_4H_{10}) is a 'butterfly'-shaped, *arachno*. The longer B–B interactions along the wings are characterized by lower bond orders (β_{BB} = 0.37) than that for the cross-linking interaction (β_{BB} = 0.66). The separation of the boron atoms at the 'wing-tips' is in excess of 3 Å with a negligible bond order. Tetraborane(10) is stabilized by six 3c-2e bonds. The strongest of these interactions (β_{BH_bB} = 0.13) are four symmetry-equivalent B–H_b–B three-centre bonds along the butterfly wings. Two slightly weaker (β_{BBB} = 0.12) three-centre interactions are also detected for the wings. Although only slightly weaker than the other three-centre interactions discussed above, they have not conventionally been included in descriptions of the bonding in this molecule. Fig. 1(d) shows the calculated molecular diagram including all of these interactions.

Heptaborane(7), $B_7H_7^{2-}$, is predicted to be a pentagonal biprismatic *closo* borane, in agreement with solution NMR data.[47] The shorter separation of the equatorial boron atoms leads to a larger bond order (β_{BB} = 0.82) compared to that to the axial sites (β_{BB} = 0.53). Ten symmetry equivalent 3c-2e bonds are detected for the B_{eq}–B_{ax}–B_{eq} triangles (β_{BBB} = 0.14). No other significant three-centre interactions are found so that the molecular diagram in Fig. 1(e) is very similar to that for $B_6H_6^{2-}$ with the cluster bonding lying on the *pseudo*-spherical surface.

Hexaborane(10), B_6H_{10}, is a pentagonal pyramidal, *nido* borane. The unbridged B_{eq} atoms interact with a much higher bond order (β_{BB} = 0.96) than for the bridged connections (β_{BB} = 0.40–0.50) due to the absence of H_b atoms. The apical boron atom interacts with the B_{eq} atoms with bond orders (β_{BB} = 0.60–0.48) which decrease as the number of H_b atoms on B_{eq} atoms increases.

Conversely, the five 3c-2e B_3 interactions detected for the triangular faces of the pyramid have bond orders (β_{BBB} = 0.17–0.12) which *increase* with the number of H_b atoms attached to the B_{eq} atoms involved. Four further three-centre interactions are detected corresponding to the B_{eq}–H_b–B_{eq} interactions. The molecular diagram in Fig. 1(f) is thus very similar to that in the *nido* B_5H_9.

Pentaborane(11), B_5H_{11}, is an *arachno* borane with a 'butterfly' structure that has two B atoms in 'wing-tip' positions, two B atoms in 'body' positions and the apical boron at the 'head' position. The bond orders (β_{BB} = 0.44) between the apical and 'wing-tip' boron atoms are quite similar to those for the interactions between the 'wing-tip' and 'body' atoms and are actually larger than for the interaction between the two atoms in 'body' positions (β_{BB} = 0.37) despite being *ca.* 0.1 Å longer than either. The apical–'body' separation is slightly shorter but is associated with a much higher bond order (β_{BB} = 0.59). The higher than expected bond orders associated with interactions with the apical boron are coupled to the lower positive charge on this site. Three 3c-2e B_3 interactions are detected with the two strongest involving the apical, 'wing tip' and 'body' boron positions (β_{BBB} = 0.16) and the third connecting the apical and 'body' boron atoms (β_{BBB} = 0.12). Four 3c-2e bonds involving bridging hydrogen atoms are detected. Three of these are between boron atoms in conventional μ-bridging positions.

The remaining three-centre bond is unusual, in that it involves a hydrogen atom that on casual inspection would seem to lie in a terminal position. It involves one of the boron atoms at the 'wing-tip' positions, the apical boron atom and the hydrogen atom bound to the apical boron atom. The three-centre interaction is very asymmetric, with the hydrogen atom *ca.* 0.2 Å closer to the apical boron atom. No doubt, this asymmetry accounts for the relatively weak three-centre bond order (β_{BHB} = 0.13) but this is in the range normally considered significant.[28] This interaction has been proposed previously[48,49] and recent gas-phase electron diffraction data supports the highly asymmetric interaction.[50] The three-centre bond order for the interaction of this hydrogen atom with the other 'wing-tip' boron atom is negligible. The alternative arrangement in which the hydrogen atom is connected to both 'wing-tip' positions as well as the apical boron atom leads to two slightly smaller bond orders (β_{BHB} = 0.10) and is, in fact, a transition state.

The molecular diagram, shown in Fig. 1(g), thus shows additional features to that on the conventional structural representation[44] of this cluster. The additional three-centre term, which might be termed an agostic interaction in a metal cluster, illustrates the fine line that exists between what is and is not a bond in complex bonding cases such as the boranes.

Housecroft *et al.*[42] assert that cross-polyhedral B–B bond orders should be considered insignificant, at least in the *closo* boranes. Though small cross-polyhedral bonding interactions (β_{BB} = 0.15) are found in $B_6H_6^{2-}$, such interactions are much smaller in $B_7H_7^{2-}$ (β_{BB} = 0.05 for axial–axial and β_{BB} = 0.08 for *cis*-related equatorial–equatorial). In higher boranes, where the separations are larger, such interactions are inconsequential. Bochicchio *et al.*[46] assert that three-centre bonds in molecules are strictly localized to certain regions, whereas the rest of the

molecule can be described by classical 2c-2e bonds. This assessment is certainly applicable to all of the boranes examined here, and by extension is presumably the case in larger boranes also. The 3c-2e bonds tend to be located on the surface described by the B–B–B and B–H_b–B groups so that the skeletal electron density is close to the *pseudo*-spherical surfaces on which the boron atoms lie in the *closo* boranes[25,42,43,51,52] and on the remaining surface in the *nido* and *arachno* species.

Multicentre bonding in electron-rich compounds

A. Xenon fluorides

The presence of 3c-4e bonding in the xenon fluorides has long been predicted[53] and thus these systems serve as a useful test set. The optimized and available experimental structures are given in the ESI.†

The Xe–F bond order (β_{XeF} = 0.41) in linear XeF_2 arises almost completely from σ-bonding; the π component of the bond order is negligible. The three-centre F–Xe–F bond order (β_{FXeF} = −0.25) indicates both a high degree of delocalization and the presence of a 3c-4e bond. This arises from a σ_u molecular orbital of the form shown in Scheme 3. The fluorine atoms reach a total valency close to one (calculated using the definition in eqn (2)) due to the large ionic component associated with high partial charges on the atoms (q_F = −0.6). The presence of a 3c-4e bond seems unequivocal from the molecular orbitals and from the bond order analysis.

From an electron localization function analysis, Silvi suggests[18] that there is no 3c-4e bond in XeF_2 (and, by extension, in any other system) because the electron localization function does not show the same behaviour exhibited by 3c-2e bonded systems. It should be noted, however, that 3c-4e bonds are intrinsically different from 3c-2e bonds in that, as described in the Introduction, they *can* be localized but only into functions which provide half bonds.

The bonding in the square planar XeF_4 and approximately octahedral XeF_6 is very similar to that in XeF_2. There is a small increase in the Xe–F bond order (β_{XeF} = 0.45 and 0.50, respectively). Two 3c-4e interactions are detected in XeF_4 (β_{FXeF} = −0.24) and three are detected in XeF_4 (β_{FXeF} = −0.20) and each involve *trans* related F atoms only. In both cases these arise from molecular orbitals of the type implicated in XeF_2. Three-centre interactions involving *cis* related F atoms are small.

The cations XeF_3^+ and XeF_5^+ have structures which are related to those of XeF_2 and XeF_4 by the addition of a *cis* related F atom. Bond contraction from the positive charge leads to slightly higher bond orders ($\beta_{XeF} \sim 0.6$). In both cases, the 3c-4e bonds in the parent molecules are preserved and no additional terms involving the *cis*-related group are introduced.

3c-4e interactions are detected and are important in all of the xenon fluorides and arise from σ-overlap of a Xe p-orbital with F orbitals, as illustrated in Scheme 3 within each linear {XeF_2} subunit. These triatomic subunits are essentially singly bonded.

B. Polyoxometalates

This large class of compounds is commonly based on high-oxidation, group 5 or 6 metal–oxygen clusters with edge-sharing MO_4 or MO_6 polyhedra arranged such that they form enclosed and often highly symmetrical structures. We have recently published a number of papers[20,21,54,55] aimed at developing an understanding of the bonding in these complex species. It has been proposed[56–59] that metal–oxygen rings in polyoxometalates, termed 'closed loops', be regarded as a delocalized bonding system featuring interpenetrating loops of σ- and π-type orbitals. In this section, the presence and importance of such delocalization is analyzed in a representative set of molybdates (four Lindqvist anions, β-octamolybdate, an Anderson-type tellurohexamolybdate and a Keggin phosphododecamolybdate). The Lindqvist and Keggin structures contain only one terminal oxo group per metal atom, and are thus categorized as Type I polyoxometalates, whereas the octamolybdate and Anderson structures have metal atoms with two terminal oxo groups, and are thus categorized as Type II systems. The Lindqvist and octamolybdate anions contain only group 5 and 6 metal ions and are examples of isopolyanions whereas the Anderson and Keggin anions also contain heteroatoms and are classified as heteropolyoxometalates. We have previously investigated other aspects of the bonding in these systems and the optimized and experimental structures are given in the original computational papers.

The structure of the Lindqvist isopolyanion $Mo_6O_{19}^{2-}$, shown in Fig. 2(a), consists of edge-sharing, distorted {MoO_6} units with each Mo(VI) ion bonded to a single terminal oxo group (O_t), four two-coordinate bridging oxygen atoms (O_b) and a six-coordinate oxygen atom (O_c) that occupies the centre of the O_h cluster.

Three equivalent closed loops have been proposed[57] for these anions based on the eight-membered {Mo_4O_4} planar rings that lie perpendicular to the molecular C_4 axes. We have previously identified σ and π molecular orbitals possessing this loop structure[54] and Cai *et al.*[60] have suggested the presence of aromatic character in the loops due to Mo–O_b d_π–p_π interactions. The three-centre analysis reveals twenty-four 3c-4e bonds ($\beta_{O_tMoO_b}$ = −0.09) which combine, as shown in Fig. 3(a), to make up such loops. Whilst the sign of the bond order is indicative of a 3c-4e interaction, its small magnitude suggests only a weak delocalization. This is consistent with our previous conclusion,[54] based on an energy decomposition analysis, that the closed-loops are present but do not stand out as a stabilizing factor. Fig. 2(a) shows the molecular diagram for this anion and neatly summarizes the considerable differences in the natures of the Mo–O_t, Mo–O_b and Mo–O_c interactions. Our previous analysis of closed-loops has been restricted to this system which, due to its high symmetry, is amenable to detailed analysis. The present methodology is not restricted in this way.

Reduction to give $Mo_6O_{19}^{3-}$ leads to occupation of a doubly-degenerate, delocalized Mo–O_b π-antibonding orbital with the resulting ^2E_u state subject to a small Jahn–Teller distortion.[54,61] The delocalized nature of the singly occupied orbital leads to minor changes in bond lengths and a reduction in the 3c-4e bond order in the degenerate ^2E_u state as well as in the Jahn–Teller distorted $^2A_2$ and $^2B_2$ states.

Substitution of a Mo(VI) atom in the fully oxidized anion for a Nb(V) atom leads to the C_{4v} $NbMo_5O_{19}^{3-}$ anion in which the two loops of weak 3c-4e bonds passing through the

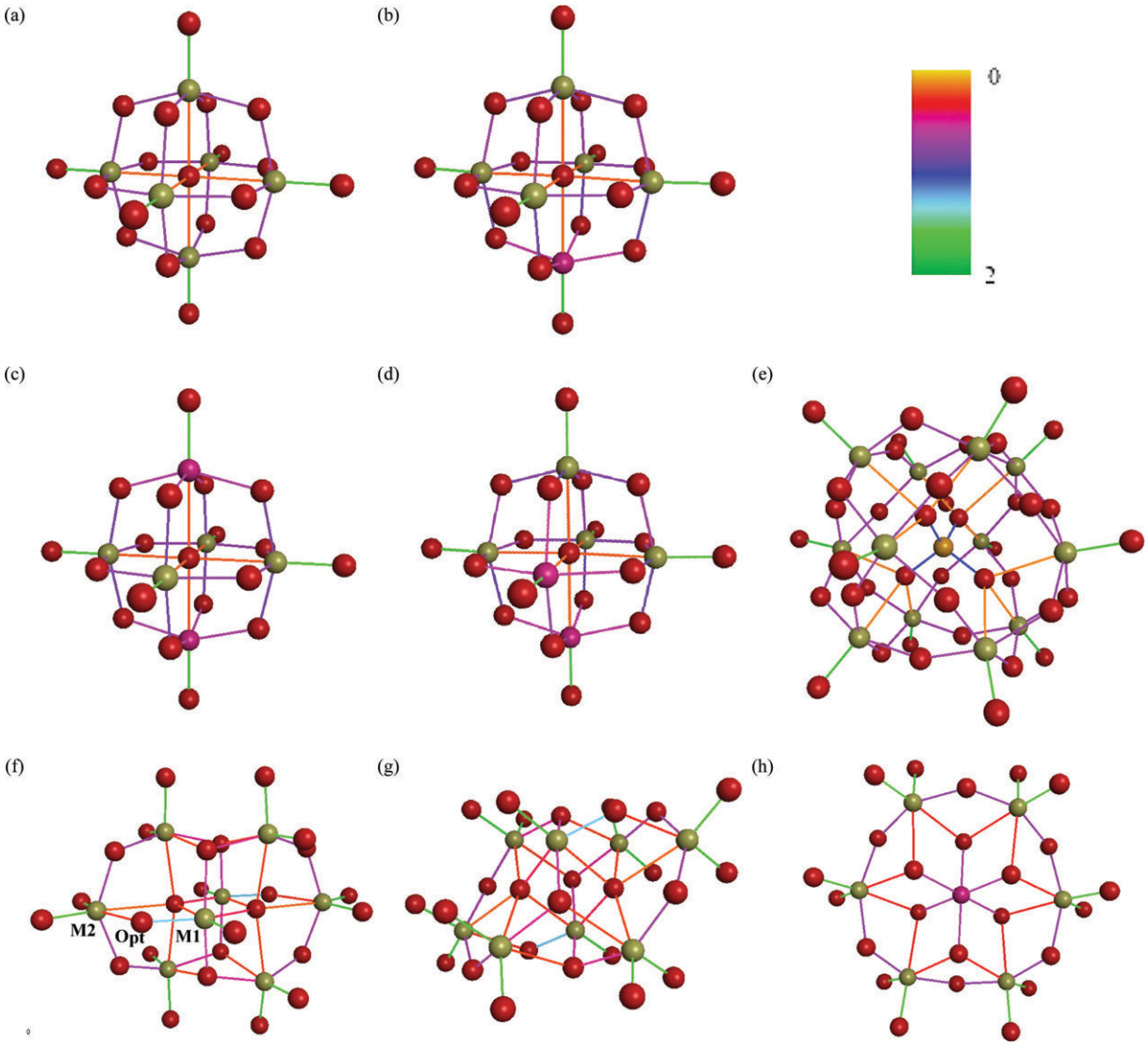

Fig. 2 Molecular diagrams for (a) $Mo_6O_{19}^{2-}$ (b) $NbMo_5O_{19}^{3-}$, (c) *trans*-$Nb_2Mo_5O_{19}^{4-}$, (d) *cis*-$Nb_2Mo_5O_{19}^{4-}$, (e) α-$PMo_{12}O_{40}^{3-}$, (f) β-$Mo_8O_{26}^{4-}$ (showing bicapped ring of $\{Mo_6O_{18}\}$), (g) β-$Mo_8O_{26}^{4-}$ (showing two $\{Mo_4O_{12}\}$ subunits) and (h) $TeMo_6O_{24}^{6-}$ showing two-centre bond orders as coloured lines using the colour scale shown and Mo (green), O (red), Nb (purple), P (gold) and Te (purple).

heteroatom are weakened by the lower covalency associated with its lower charge. This is evident in the molecular diagram, shown in Fig. 2(b). The bonding in the remaining $\{Mo_4O_4\}$ loop is slightly enhanced ($\beta_{O_tMoO_b} = -0.11$) and Fig. 3(b) shows how the presence of three-centre interactions leads to the loop structure. A second such substitution gives rise to either *cis* or *trans* $Nb_2Mo_4O_{19}^{4-}$ polyanion. In the *trans* isomer, there is further enhancement of the Mo–O bonding, as shown in the molecular diagram in Fig. 2(c), and loss of any delocalization along the two loops containing the Nb(v) atoms. The remaining loop, shown in Fig. 3(c), involves only molybdenum and oxygen atoms with the same 3c-4e bond order as in the singly substituted anion. In the C_{2v} *cis* isomer, there is additional enhancement of the Mo–O bonding, as shown in the molecular diagram in Fig. 2(d), and disruption of all three loops, as shown in Fig. 3(d).

α-$PMo_{12}O_{40}^{3-}$ has the Keggin structure[62] with the ideal T_d symmetry shown in the molecular diagram shown in Fig. 2(e). The single oxo group on each Mo atom has a considerable *trans* influence. One of the four equivalent $\{Mo_6O_6\}$ loops which can be constructed through the interaction between the metal and two-coordinate oxygen atoms is clear in this figure. The three-centre interactions, shown in Fig. 3(e), match this topology and are of very similar magnitude ($\beta_{O_tMoO_b} \sim -0.1$) to those in the other proposed loops. No involvement from the heteroatom is apparent in these loops.

Reduction to form α-$PMo_{12}O_{40}^{4-}$ leads to occupation of a doubly degenerate π-antibonding orbital with the ^2E state subject to a small Jahn–Teller distortion and a C_s ground state. As in the Lindqvist anion, reduction is accompanied by a disruption of the three-centre interactions.

The C_{2h} octamolybdate isomer, β-$Mo_8O_{26}^{4-}$, contains three types of nominally six-coordinate molybdenum atoms. The molecular diagram, shown in Fig. 2(f) and (g), illustrates the complexity of the variations in the bond orders, and the subtle distinction between possible descriptions of the metal

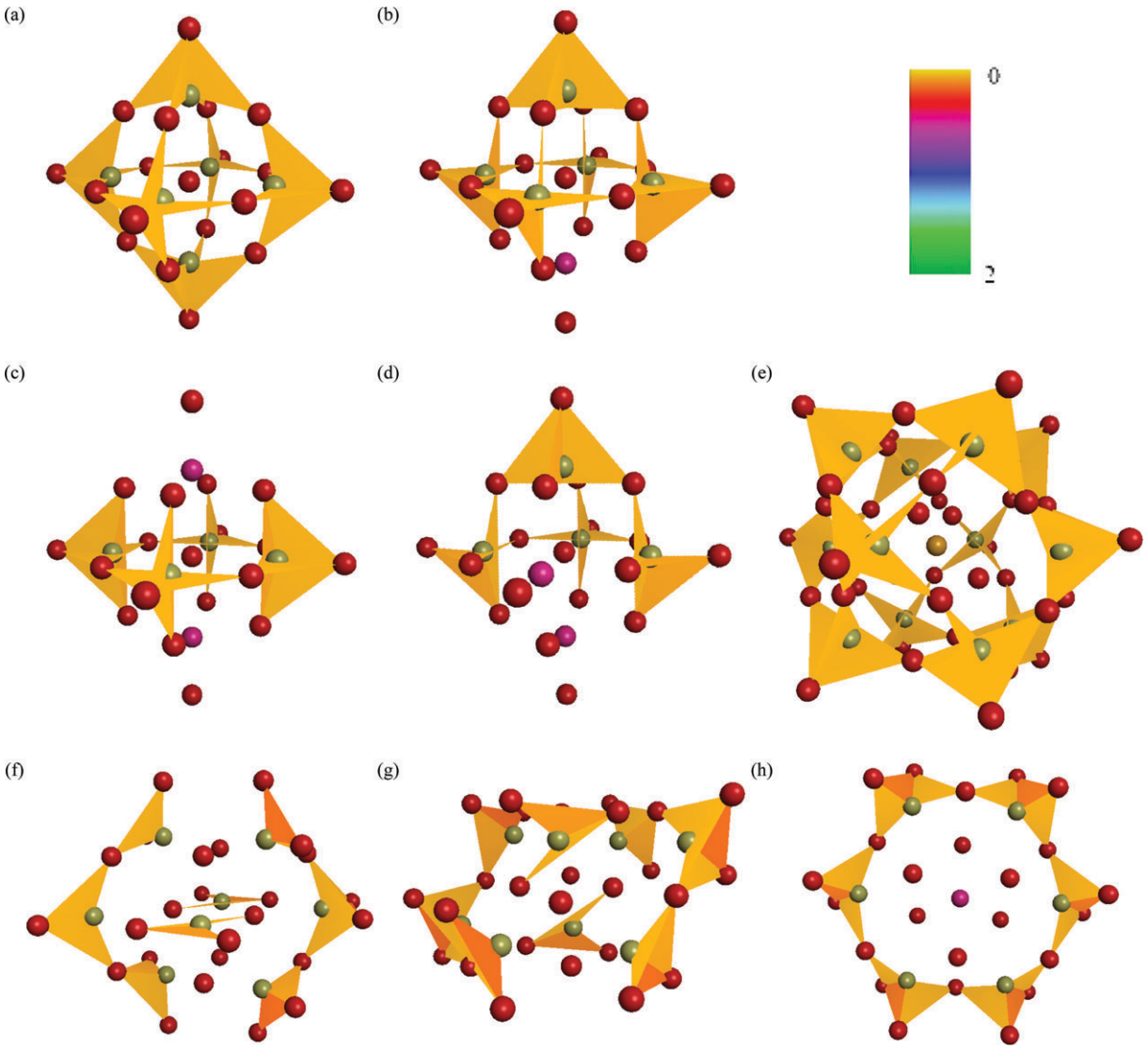

Fig. 3 Molecular diagrams for (a) $Mo_6O_{19}^{2-}$ (b) $NbMo_5O_{19}^{3-}$, (c) *trans*-$Nb_2Mo_5O_{19}^{4-}$, (d) *cis*-$Nb_2Mo_5O_{19}^{4-}$, (e) α-$PMo_{12}O_{40}^{3-}$, (f) β-$Mo_8O_{26}^{4-}$ (showing bicapped ring of $\{Mo_6O_{18}\}$), (g) β-$Mo_8O_{26}^{4-}$ (showing two $\{Mo_4O_{12}\}$ subunits) and (h) $TeMo_6O_{24}^{6-}$ showing three-centre bond orders as coloured lines using the colour scale shown and Mo (green), O (red), Nb (purple), P (gold) and Te (purple).

polyhedra. Fig. 2(f) shows the structure as a ring of six, edge-sharing $\{MoO_6\}$ with two capping $\{MoO_6\}$ units whilst Fig. 2(g) shows the structure as two offset $\{Mo_4O_{12}\}$ ring subunits, with the molybdenum atoms arranged in an approximate diamond.

The analysis suggests that whilst the M1–O_{pt} interaction is characteristic of a multiply bonded oxo group, the weak M2–O_{pt} bond is real and so the description of this oxygen atom as *pseudo*-terminal or even bridging is appropriate, despite the M1–O_{pt} and M1–O_t bonds being structurally comparable.

The presence of two, eight-membered $\{Mo_4O_4\}$ closed loops has been proposed by Nomiya and Miwa[57] in β-octamolybdate. Although these authors did not identify the location of the loops, they presumably involve the two $\{Mo_4O_{12}\}$ rings shown in Fig. 2(g). Fig. 3(f) and (g) show the calculated 3c-4e interactions, from the same viewpoints as Fig. 2(f) and (g), respectively. Three-centre interactions of comparable magnitude to those detected in the Lindqvist anions ($\beta_{O_tMoO_b} \sim -0.1$) are found within the loops in the $\{Mo_4O_{12}\}$ rings. More significant three-centre interactions ($\beta_{O_tMoO_t} \sim -0.2$), involving each of the *cis*-related O_t–Mo–O_t in this Type II polyanion are detected.

The Anderson structure,[62] exemplified by $TeMo_6O_{24}^{6-}$, contains a ring of six, distorted $\{MoO_6\}$ connected by two- and three-coordinate O_b atoms and a central heteroatom which is coordinated to all six of the three-coordinate O_b atoms. As in β-octamolybdate, the Mo atoms are each bonded to two, *cis*-related oxo atoms. The molecular diagram, shown in Fig. 2(h), neatly summarizes the variations in the internal bonding and the distinct and distinctive *trans* influence of the oxo groups.

$\{Mo_6O_6\}$ closed loops involving all of the Mo atoms have been proposed.[57] These loops are constructed from three-centre interactions of comparable magnitude to those detected in the other polyoxometalates ($\beta_{O_tMoO_b} \sim -0.1$). As found for

Scheme 4 3c-4e O_t–M–O_t p_π–d_π–p_π bond in *cis*-MO_2^{2+} unit.

the other Type II system studied, β-octamolybdate, stronger 3c-4e interactions are predicted ($\beta_{O_tMoO_t} \sim -0.2$) involving each of the *cis*-related O_t–Mo–O_t groups. Fig. 3(h) shows the calculated three-centre interactions.

Although the {TeO_6} octahedron at the centre of the ion is strongly bound to the surrounding ring, these are primarily located bonds as no multicentre bonds mediated by the tellurium atom are detected.

The polyoxometalates studied exhibit weak 3c-4e bonding. O_t–Mo–O_b interactions are characterized in each system by similar bond orders ($\beta_{O_tMoO_b} \sim -0.1$) which, although small, do correspond to the closed loops suggested by Nomiya and Miwa[56–58] and by King[59] and identified in our previous molecular orbital descriptions[20,21,54,55] of these systems. The magnitude of these bond orders is on the limit of what can be considered indicative of a bond. Nevertheless, the bond orders are very similar in each system and decrease in the reduced and substituted systems in a manner that would be anticipated from bonding considerations. Although small, the three-centre bond orders are still considerably larger than those obtained for systems such as CCl_4 ($\beta_{ClCCl} < -0.05$) and $SiCl_4$ ($\beta_{ClSiCl} < -0.05$) in which no delocalization is expected.

The bonding involving the heteroatom in heteropolyoxometalates appears to be localized. In Type II polyanions, somewhat stronger 3c-4e interactions ($\beta_{O_tMoO_t} \sim -0.2$) involving each of the *cis*-related O_t–Mo–O_t groups are detected. The relatively strong 3c-4e interaction is due to the interaction pictured in Scheme 4 and is an important contribution[63] to the stronger Mo–O_t bonding that is possible in *cis*-related O_t–Mo–O_t groups compared to the *trans* form. That the d_π–p_π 3c-4e bonding favours a 90° interaction should be contrasted with the 180° interaction favoured by the p_σ–p_σ 3c-4e bonding in the xenon fluorides.

Conclusions

In many ways the Lewis model of electron-pair bonding has survived the advent of quantum mechanics with the pairs being replaced by doubly occupied molecular orbitals or localized 'bond orbitals'. Whilst localization of the multicentre molecular orbitals obtained from high-level electronic structure calculations is possible in most cases, the electronic structure of molecules where this is not possible, including electron-deficient and electron-rich molecules is often chemically very interesting. Three-centre bond orders provide a useful tool for detecting the presence and analyzing the importance of multicentre and hypervalent effects but have had limited use in all but small molecules. To assist in the detection of multicentre interactions and to stimulate further investigations in larger systems, a graphical device is introduced which constructs the chemical connections *ab initio* from the electronic structure. The three-centre, two-electron bonding in a set of electron-deficient boranes and the three-centre, four-electron bonding in a set of electron-rich xenon fluorides has been analyzed using this method, to map the occurrence and network of the multicentre interactions. The approach has been used to detect multicentre effects in polyoxometalates for the first time. The previously suggested *pseudo*-aromatic, closed-loops in these large systems polyoxometalates have been detected but are found to be relatively weak in magnitude.

References

1. W. N. Lipscomb, *Boron Hydride Chemistry*, Academic Press, New York, 1975.
2. R. E. Dickerson and W. N. Lipscomb, *J. Chem. Phys.*, 1957, **27**, 212.
3. W. N. Lipscomb, *Acc. Chem. Res.*, 1973, **8**, 257.
4. L. Pauling, *The Nature of the Chemical Bond*, Cornell University Press, New York, 1960.
5. K. Wade, *Electron Deficient Compounds, Studies in Modern Chemistry*, Nelson, London, 1971.
6. H. C. Longuet and J. Higgins, *J. Chim. Phys. Phys. Chim. Biol.*, 1949, **46**, 275.
7. G. N. Lewis, *J. Am. Chem. Soc.*, 1916, **38**, 762.
8. I. Langmuir, *J. Am. Chem. Soc.*, 1919, **41**, 868.
9. A. J. Bridgeman, G. Cavigliasso, L. R. Ireland and J. Rothery, *J. Chem. Soc., Dalton Trans.*, 2001, 2095.
10. A. J. Bridgeman and C. J. Empson, *Chem.–Eur. J.*, 2006, **12**, 2252.
11. J. N. Murrell, S. F. A. Kettle and J. M. Tedder, *The Chemical Bond*, John Wiley & Sons, Chichester, 1978.
12. M. S. de Giambiagi, M. Giambiagi and M. de Souza Fortes, *J. Mol. Struct. (Theochem)*, 1997, **391**, 141.
13. A. S. Mikhaylushkin, J. Nylén and U. Häussermann, *Chem.–Eur. J.*, 2005, **11**, 4912.
14. A. B. Sannigrahi, P. K. Nandi, L. Behara and T. Kar, *THEOCHEM*, 1992, **95**, 259.
15. M. Giambiagi, M. S. de Giambiagi, C. D. dos Santos Silva and A. P. de Figueiredo, *Phys. Chem. Chem. Phys.*, 2000, **2**, 3381.
16. C. G. Bollini, M. Giambiagi, M. S. de Giambiagi and A. P. de Figueiredo, *Struct. Chem.*, 2001, **12**, 113.
17. R. F. W. Bader, *Atoms in Molecules: A Quantum Theory*, Oxford University Press, Oxford, 1990.
18. B. Silvi, *J. Mol. Struct.*, 2002, **614**, 3.
19. T. Kar and S. Scheiner, *THEOCHEM*, 1996, **370**, 45.
20. A. J. Bridgeman and G. Cavigliasso, *J. Phys. Chem. A*, 2003, **107**, 4568.
21. A. J. Bridgeman and G. Cavigliasso, *Faraday Discuss.*, 2003, **124**, 239.
22. I. Mayer, *Chem. Phys. Lett.*, 1983, **97**, 270.
23. I. Mayer, *Int. J. Quantum Chem.*, 1984, **26**, 151.
24. K. A. Wiberg, *Tetrahedron*, 1968, **24**, 1083.
25. D. R. Armstrong, P. G. Perkins and J. J. P. Stewart, *J. Chem. Soc., Dalton Trans.*, 1973, 838.
26. R. A. Evarestov and V. A. Veryazov, *Theor. Chim. Acta*, 1991, **81**, 95.
27. M. Giambiagi, M. S. de Giambiagi and K. C. Mundim, *Struct. Chem.*, 1990, **1**, 423.
28. A. B. Sannigrahi and T. Kar, *Chem. Phys. Lett.*, 1990, **173**, 569.
29. R. Ponec and I. Mayer, *J. Phys. Chem. A*, 1997, **101**, 1738.
30. A. B. Sannigrahi and T. Kar, *Chem. Phys. Lett.*, 1999, **299**, 518.
31. A. B. Sannigrahi and T. Kar, *THEOCHEM*, 2000, **496**, 1.
32. R. L. De Kock and W. B. Bosma, *J. Chem. Educ.*, 1988, **65**, 194.
33. R. Ponec, G. Yuzhakov and D. L. Cooper, *Theor. Chem. Acc.*, 2004, **112**, 419.
34. A. D. Becke, *Phys. Rev. A: At., Mol., Opt. Phys.*, 1988, **38**, 3098.
35. J. P. Perdew, *Phys. Rev. B: Condens. Matter Mater. Phys.*, 1986, **33**, 8822.
36. J. P. Perdew, *Phys. Rev. B: Condens. Matter Mater. Phys.*, 1986, **34**, 7406.
37. C. Fonseca Guerra, J. G. Snijders, G. te Velde and E. J. Baerends, *Theor. Chem. Acc.*, 1998, **99**, 391.

38. G. te Velde, F. M. Bickelhaupt, S. J. A. van Gisbergen, C. Fonseca Guerra, E. J. Baerends, J. G. Snijders and T. Ziegler, *J. Comput. Chem.*, 2001, **22**, 931.
39. *ADF2003.01*, SCM, Theoretical Chemistry, Vrije Universiteit, Amsterdam, The Netherlands, 2003, http://www.scm.com.
40. A. J. Bridgeman and C. J. Empson, *MAYER*, The University of Sydney, Sydney, Australia, 2007, http://assign3.chem.usyd.edu.au/bond_orders.
41. A. J. Bridgeman and C. J. Empson, *MAYER VISUALIZER*, The University of Sydney, Sydney, Australia, 2007, http://assign3.chem.usyd.edu.au/bond_orders.
42. C. E. Housecroft, C. Snaith, K. Moss, R. E. Mulvey, M. E. O'Neill and K. Wade, *Polyhedron*, 1985, **4**, 1875.
43. D. R. Armstrong, P. G. Perkins and J. J. P. Stewart, *J. Chem. Soc., Dalton Trans.*, 1973, 627.
44. K. Wade, *Adv. Inorg. Chem. Radiochem.*, 1976, **18**, 1.
45. R. E. Williams, *Inorg. Chem.*, 1971, **10**, 210.
46. R. C. Bochicchio, R. Ponec, L. Lain and A. Torre, *J. Phys. Chem. A*, 1998, **102**, 7176.
47. F. Klanberg, D. R. Eaton, L. J. Guggenberger and E. L. Muetterties, *Inorg. Chem.*, 1967, **6**, 1271.
48. P. V. Schleyer, M. Buhl, U. Fleischer and W. Koch, *Inorg. Chem.*, 1990, **29**, 153.
49. R. E. Williams, *Chem. Rev.*, 1992, **92**, 177.
50. P. T. Brain, D. Hnyk, D. W. H. Rankin, M. Buhl and P. V. Schleyer, *Polyhedron*, 1994, **13**, 1453.
51. C. E. Housecroft, *Polyhedron*, 1985, **4**, 1875.
52. E. L. Muetterties, *Boron Hydride Chemistry*, Academic Press, New York, 1975.
53. T. A. Albright, J. K. Burdett and M.-H. Whangbo, *Orbital Interactions in Chemistry*, Wiley, New York, 1985.
54. A. J. Bridgeman and G. Cavigliasso, *Inorg. Chem.*, 2002, **41**, 1761.
55. A. J. Bridgeman, *J. Phys. Chem. A*, 2002, **106**, 12151.
56. K. Nomiya, *Polyhedron*, 1987, **6**, 309.
57. K. Nomiya and M. Miwa, *Polyhedron*, 1984, **3**, 341.
58. K. Nomiya and M. Miwa, *Polyhedron*, 1985, **4**, 89.
59. R. B. King, *Inorg. Chem.*, 1991, **30**, 4437.
60. T. Cai, Z. D. Chen, X. Z. Wang, L. M. Li and J. X. Lu, *Prog. Nat. Sci.*, 1997, **7**, 554–561.
61. A. J. Bridgeman and G. Cavigliasso, *Chem. Phys.*, 2002, **279**, 143.
62. A. J. Bridgeman and G. Cavigliasso, *J. Phys. Chem. A*, 2003, **107**, 6613.
63. A. J. Bridgeman and G. Cavigliasso, *J. Chem. Soc., Dalton Trans.*, 2001, 3556.